ChemPubSoc Europe

DOI: 10.1002/ejic.201701363

EurJIC European Journal of Inorganic Chemistry

Full Paper

Organozinc Chemistry | *Very Important Paper* |

1,2-Addition of Diethylzinc to a Bis(Imidazolyl)ketone Ligand

Emma Folkertsma,[a] Sanne H. Benthem,[a] Johann T. B. H. Jastrzebski,[a] Martin Lutz,[b] Marc-Etienne Moret,[a] and Robertus J. M. Klein Gebbink*[a]

Abstract: In this study, the selective 1,2-addition of diethylzinc to the ketone functionality of $BM^{diPh}IK$ [bis(1-methyl-4,5-diphenylimidazolyl)ketone] is shown. The reaction product is isolated in a dimeric form with a planar $Zn_2(\mu\text{-}O)_2$-motif keeping the two monomers together. This compound can serve as a model for reactive intermediates in the catalytic alkylation of ketones with diorganozinc reagents. Hydrolysis of this binuclear zinc compound leads to isolation of the C-alkylated product in 89 % yield. A reaction pathway is proposed in which $BM^{diPh}IK$ initially coordinates to diethylzinc as a bidentate bis(nitrogen) ligand. This is followed by the homolytic cleavage of the Zn–Et bond and in-cage recombination of the Et-radical and the Zn-coordinated ligand-centered radical, which is mainly localized on the carbonyl moiety of the ligand.

Introduction

Diorganozinc reagents are widely used as selective alkylating agents for the alkylation of functionalized electrophiles in organic synthesis.[1] Furthermore, they can be used in Pd- and Ni-catalyzed cross-coupling reactions for carbon–carbon bond formation.[2] Other applications in organic synthesis are the (enantioselective) addition to aldehydes, ketones, and imines, the conjugate addition to α,β-unsaturated compounds,[3] the direct addition to alkenes and alkynes,[4,5] and as radical initiators.[6–8]

Much research has focused on the use of dialkylzinc reagents in the alkylation of aldehydes,[9–12] while the alkylation of ketones is more challenging and often a Ti- or Al-containing activator is used in the addition of diorganozinc compounds to a ketone.[13–24] Due to the possible formation of Zn-enolate compounds from α-acidic ketones or the formation of self-aldol products, the addition of organozinc compounds to ketones is often not successful.[25] Additionally, ketones are generally less reactive than aldehydes. The first literature example of the addition of an organozinc reagent (Ph_2Zn) to a ketone without the need of a Ti-activator dates from 1998 by Fu et al.,[26] while the first example using Et_2Zn by Ishihara et al., dates only from 2007.[27] Both examples make use of catalytic amounts of an organic ligand. Ishihara et al. used chiral phosphoramide–Zn^{II} complexes as conjugate acid–base catalysts for enantioselective organozinc C-addition to ketones (vide supra). On the other hand, Fu et al. used 3-*exo*-(dimethylamino)isoborneol (DAIB) in the presence of MeOH as chiral catalyst for the enantioselective addition of $ZnPh_2$ to a range of aryl-alkyl and dialkyl ketones. In the past decade more examples of the addition of Et_2Zn to ketones have been reported, including enantioselective examples.[25,28–31] Typically, only catalytic amounts of (chiral) ligand are used, while stoichiometric amounts of alkylzinc are needed and generally only one of the alkyl ligands is successfully transferred to the substrate.

Ishihara et al. proposed a polar mechanism for the catalytic enantioselective ethylation of ketones with Et_2Zn.[27] The transition state of this mechanism involves two zinc centers, of which one activates the incoming ketone and is coordinated to the chiral ligand, while the other acts as the alkyl transfer reagent. Lewis acid–base interactions between the catalytic zinc center and the carbonyl group of the ketone substrate and between the P=O moiety of the phosphoramide ligand and the Et_2Zn zinc center bring the reagents in close proximity and in the right orientation for alkyl transfer to take place (Figure 1, left).

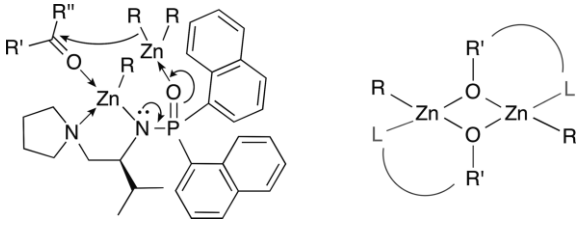

Figure 1. Left: Proposed transition state for the catalytic enantioselective ethylation of ketones with Et_2Zn.[27] Right: Schematic representation of the $Zn_2(\mu\text{-}O)_2$-motif.

The catalytic addition of an alkylzinc to a carbonyl moiety most likely leads to the formation of zinc alkoxide intermediates, which are generally not isolated. In the presence of potentially multi-electron donating alkoxide groups, three-coordinate

[a] *Organic Chemistry & Catalysis, Debye Institute for Nanomaterials Science, Utrecht University, Universiteitsweg 99, 3584 CG Utrecht, The Netherlands*
E-mail: r.j.m.kleingebbink@uu.nl
https://www.uu.nl/staff/rjmkleingebbink
[b] *Crystal and Structural Chemistry, Bijvoet Center for Biomolecular Research, Utrecht University, Padualaan 8, 3584 CH Utrecht, The Netherlands*
Supporting information and ORCID(s) from the author(s) for this article are available on the WWW under https://doi.org/10.1002/ejic.201701363.

zinc compounds tend to aggregate via oxygen bridges to attain the preferred tetrahedral geometry around the zinc center. This aggregation can lead to the formation of a central planar $Zn_2(\mu\text{-}O)_2$-motif (Figure 1, right), which is a very common structural motif for which many solid-state structures have been determined, while the formation of higher aggregates is also observed.[32]

In 2012, Okuda et al. isolated a dimeric zinc complex with an $Zn_2(\mu\text{-}O)_2$-motif from the 1,2-addition of diallylzinc to benzophenone, showing that one of the allyl-ligands adds to the ketone moiety and one remains bound to zinc.[33] This provided the first example of an isolated Zn-containing product from the 1,2-addition of an organozinc compound to a ketone. The dimeric complex is structurally related to the proposed intermediate of the addition of alkylzinc to carbonyls (Scheme 1A).

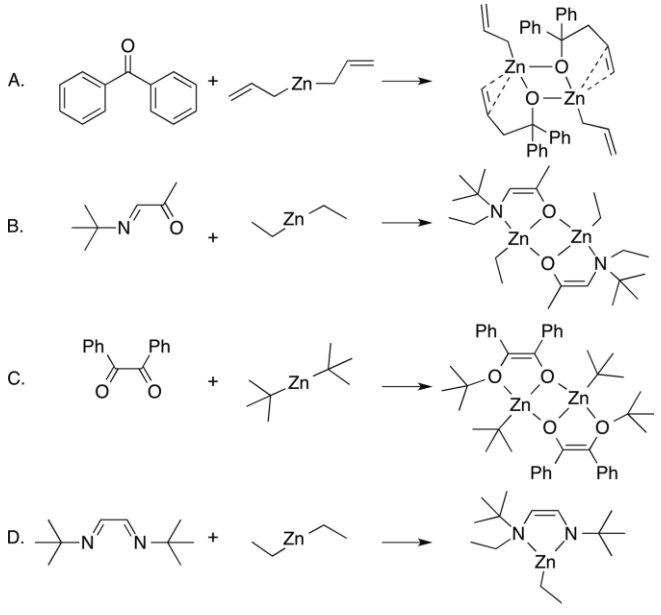

Scheme 1. A. The 1,2-addition of allylzinc to benzophenone.[33] B. Radical 1,4-addition of Et_2Zn to an α-iminoketone.[34] C. Radical addition of tBu_2Zn to dibenzoyl.[28] D. Radical 1,4-addition of Et_2Zn to an α-diimine.[36]

While a polar mechanism is proposed for the addition of alkylzinc reagents to carbonyls, radical mechanisms are generally proposed for 1,4-addition reactions, as confirmed by EPR studies.[34,35] Spek et al. have reported on the 1,4-addition of Et_2Zn to an α-iminoketone leading to *N*-alkylation (Scheme 1B).[34] For the 1,4-addition of Et_2Zn to dibenzoyl (dbz), leading to the *O*-alkylated product, Lewinski et al. also proposed a radical mechanism (Scheme 1C).[28] In this reaction, a minor amount of the 1,2-addition product (C-alkylation) was also observed.[28] Both radical 1,4-addition reactions result in the formation of dimeric zinc complexes with a $Zn_2(\mu\text{-}O)_2$-motif (Scheme 1). Another example of a 1,4-addition is the addition of alkylzinc reagents to α-diimines (Scheme 1D).[36] For this reaction extensive mechanistic studies were performed leading to the proposal of an inner sphere single electron transfer (SET) mechanism.[36,37] In contrast to the first three examples, the product of the last example is isolated as the monomer because of the lack of multi-electron donating alkoxide groups.

Here, the stoichiometric reactivity of the bidentate *N*,*N*-ligand $BM^{diPh}IK$ [bis(1-methyl-4,5-diphenylimidazolyl)ketone] with Et_2Zn is reported (Scheme 2). With its potentially coordinating nitrogen and carbonyl moieties, this ligand shows similarities to α-iminoketones as well as α-diimines for which 1,4-addition of Et_2Zn leading to *N*-alkylation is observed.[28,34,35,38,39] However, also addition to the ketone, leading to C-alkylation is plausible. Because both α-carbons relative to the carbonyl functionality in the $BM^{diPh}IK$ ligand lack a proton, the formation of the earlier mentioned Zn-enolates or self-aldol products is not possible. While there are several possible reaction pathways of $BM^{diPh}IK$ with Et_2Zn, it turns out that $BM^{diPh}IK$ undergoes a selective 1,2-addition with Et_2Zn leading to the C-alkylated product. This selectivity initiated the interest to investigate this reaction further as a stoichiometric example of the 1,2-addition of an alkylzinc reagent to a carbonyl. In this reaction $BM^{diPh}IK$ has a bifunctional character, as it is functioning both as ligand and as substrate. As pointed out above, radical pathways are proposed for 1,4-additions to α-diimines, α-iminoketones, and α-diketones. Previous results on the reduction of $BM^{diPh}IK$ show that this results in rather stable radicals,

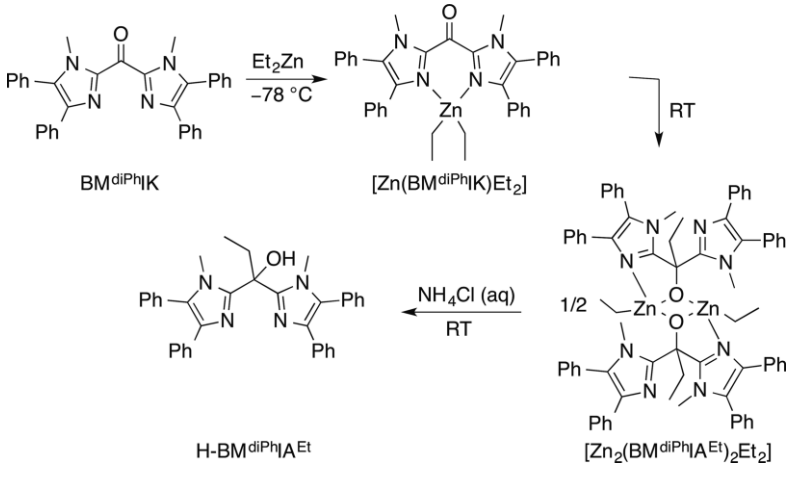

Scheme 2. The formation of the dimeric zinc complex $[Zn_2(BM^{diPh}IA^{Et})_2Et_2]$ from Et_2Zn and $BM^{diPh}IK$ via intermediate product $[Zn(BM^{diPh}IK)Et_2]$ followed by the hydrolysis of the Zn-dimer to isolate H-$BM^{diPh}IA^{Et}$.

indicating that this ligand can provide a good platform to investigate a possible radical pathway towards the alkylation of ketones.[40]

Results and Discussion

1,2-Addition of Et_2Zn to the $BM^{diPh}IK$ Ligand

Addition of a Et_2Zn solution to a suspension containing one equivalent of bis(1-methyl-4,5-diphenylimidazolyl)ketone ($BM^{diPh}IK$) in toluene at –78 °C induced an immediate color change from light yellow to dark red and complete dissolution of the ligand. This color change suggests the formation of coordination complex [Zn($BM^{diPh}IK$)Et_2] (Scheme 2) as similar colors are observed for related dialkylzinc diimine complexes.[36,41] When stirring was continued at room temperature, the color disappeared within seconds, leading to a colorless solution from which the binuclear complex [$Zn_2(BM^{diPh}IA^{Et})_2Et_2$] {$BM^{diPh}IA^{Et}$: bis(1-methyl-4,5-diphenylimidazol-2-yl)ethyl-alcohol} was obtained in 71 % yield (Scheme 2). In this reaction an uncommon 1,2-addition of Et_2Zn to the ketone in the $BM^{diPh}IK$ ligand took place. This was unambiguously proven by hydrolysis of the zinc complex and isolation of H-$BM^{diPh}IA^{Et}$ in 89 % yield (Scheme 2). The products were identified using ^1H and ^{13}C NMR, IR spectroscopy, ESI-MS, and X-ray crystal structure determination. Single crystals of [$Zn_2(BM^{diPh}IA^{Et})_2Et_2$] of high quality were obtained from a THF solution by slow vapor diffusion of hexanes.

Using IR spectroscopy, it was found that the strong ν(C=O) band at 1622 cm^{-1} for $BM^{diPh}IK$ is absent in the zinc complex indicating the formal reduction of the ketone to an alkoxide. With high-resolution mass spectrometry a molecular ion was observed at *m/z* = 1207.3925 (calcd. 1207.3948) corresponding to the binuclear product [$Zn_2(BM^{diPh}IA^{Et})_2Et$] as drawn in Scheme 2, losing one ethyl ligand. These data strongly suggest the formation of an alkoxide dimer.

This was confirmed by X-ray crystal structure determination. The molecular geometry of [$Zn_2(BM^{diPh}IA^{Et})_2Et_2$] is shown in Figure 2 and selected bond lengths and angles are given in Table 1. The structure shows the formal 1,2-addition of Et_2Zn to the carbonyl of the $BM^{diPh}IK$ ligand. The resulting dimeric zinc complex has a planar $Zn_2(\mu\text{-}O)_2$-motif with an exact, crystallographic inversion center in the middle of this motif. As a consequence of the centrosymmetry, the central $Zn_2(\mu\text{-}O)_2$ core is exactly planar and both metal atoms are equivalent. Each zinc center is coordinated by one ethyl ligand as well as an imidazole nitrogen atom and two bridging alkoxide groups, resulting in a distorted tetrahedral geometry. The angles at Zn vary between 78.11(7) and 130.00(10)°, resulting in a large angular variance of 491.24°.[44] The reason for the distortion is the ring strain in both the four- and five-membered chelate rings.

Upon the 1,2-addition a new C–C bond is formed between the ethyl groups and the original carbonyl carbons, resulting in two chiral carbon centers in [$Zn_2(BM^{diPh}IA^{Et})_2Et_2$] (as indicated in Figure 2) and the reduction of the ketones to alkoxide groups. The resulting $BM^{diPh}IA^{Et}$ ligand coordinates in an asymmetric manner with only one of the imidazole nitrogen atoms coordinating to a zinc center. The central $Zn_2(\mu\text{-}O)_2$ planar core

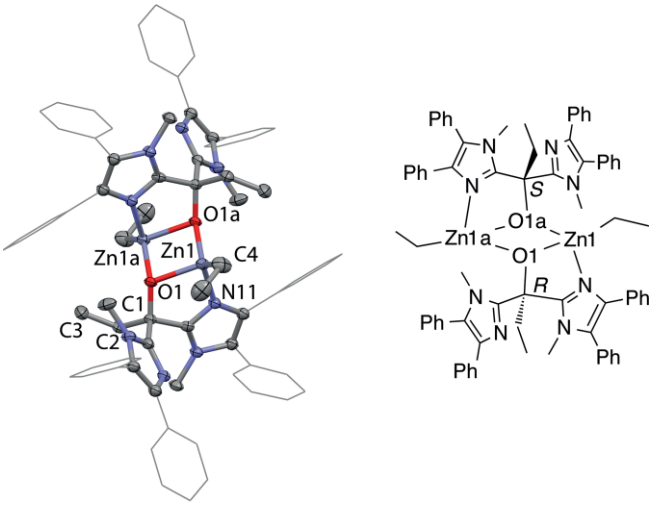

Figure 2. Left: Molecular structure of [$Zn_2(BM^{diPh}IA^{Et})_2Et_2$] in the crystal. The metal-bound ethyl group is disordered, only the major disorder component is shown. Hydrogen atoms are omitted for clarity. Displacement ellipsoids are drawn at the 40 % probability level. Right: schematic representation of [$Zn_2(BM^{diPh}IA^{Et})_2Et_2$], chiral centers are indicated with *R* and *S*.

Table 1. Selected bond lengths and angles found in [$Zn_2(BM^{diPh}IA^{Et})_2Et_2$].[a]

	Bond length (Å)		Angle (°)
Zn1–O1	2.0801(16)	O1–Zn1–O1a	87.76(6)
Zn1–O1a	2.0118(16)	Zn1–O1–Zn1a	92.24(6)
Zn1–N11	2.077(2)	O1–Zn1–N11	78.11(7)
Zn1–C4	1.972(3)	O1–Zn1–C4	123.93(11)
O1–C1	1.409(3)	N11–Zn1–C4	124.37(12)
Zn1···Zn1a	2.9497(6)	N11–Zn1–O1a	97.24(7)
O1–O1a	2.837(2)	C4–Zn1–O1a	130.00(10)

[a] Symmetry code a: 1 – *x*, 1 – *y*, 1 – *z*.

is similar to those found in previously reported complexes (vide infra), also the Zn···Zn distance of 2.9497(6) Å is similar to related compounds.[28,42,43,45] Only one example of a Zn-alkoxide isolated from a 1,2-addition to a ketone has been reported before in the literature (Scheme 1A).[33]

As mentioned before the $Zn_2(\mu\text{-}O)_2$ planar core observed here is quite a common structural motif. The majority of structures containing this motif are obtained from coordination reactions of amino alcohols with alkylzinc compounds.[35,42,43,46–54] The formation of such a Zn_2O_2-motif is often thermodynamically favored, e.g. it also forms in the reaction of O_2 with alkylzinc reagents and an external ligand; in the latter reaction O_2 is activated leading to the selective oxygenation of one Zn–C bond.[44,55] Furthermore, complexes with a planar $Zn_2(\mu\text{-}O)_2$-core are known to be active as initiator and catalyst in ring opening polymerization (ROP) reactions,[47,51,56–58] and catalytically active in, e.g., enantioselective addition of dialkylzinc compounds to aldehydes[59,60] and the asymmetric alternating copolymerization of cyclohexene oxide or oxirane and CO_2.[52,54,61]

NMR Spectroscopic Studies

The room temperature ^1H NMR spectrum of [$Zn_2(BM^{diPh}IA^{Et})_2Et_2$] shows rather broad signals, implying dynamic proc-

esses in solution on the NMR timescale. Recording the ^{1}H NMR spectrum at –30 °C results in sharpening of the signals, leading to two well-separated peaks at δ = 3.76 and 3.65 ppm, assigned to the N–CH_3 groups corresponding to an asymmetric coordination of the ligands (Figure S8, bottom). Additionally, the CCH_2CH$_3$ signals appear as complex multiplets with an ABX$_3$ pattern at δ = 3.03 and 2.89 ppm consistent with the chirality described for the crystal structure. A selective decoupling experiment by irradiating the signal for the CH$_3$-group results in a clean AB pattern at δ = 3.03 and 2.89 ppm with $^2J_{A,B}$ = 13.3 Hz for the geminal protons (inset Figure S8). Also for the ZnCH_2CH$_3$ groups an ABX$_3$ pattern is observed and a similar decoupling experiment results in the corresponding AB pattern at δ = 0.58 and 0.53 ppm with $^2J_{A,B}$ = 12.9 Hz (inset Figure S8). Using a decoupling experiment in which the signal of an ethyl CH$_2$-group is selectively irradiated, the overlapping C/Zn-CH$_2$CH_3 signals at 1.2 ppm could be distinguished. Accordingly, the triplet at δ = 1.23 ppm was assigned to ZnCH$_2$CH_3 and the triplet at δ = 1.18 ppm was assigned to CCH$_2$CH_3. These NMR spectroscopic data indicate that the geometry observed for [Zn$_2$(BM^{diPh}IA^{Et})$_2$Et$_2$] in the solid state is retained in solution at low temperature (–30 °C). Recording the ^{1}H NMR spectrum at 80 °C also results in a spectrum with sharp signals (Figures S7 and S8, top). In this spectrum only one peak for the four N–CH_3 substituents is observed at δ = 3.61 ppm, indicating a fast exchange of the coordinating and non-coordinating imidazole rings which results in a fast inversion of configuration of the chiral carbon centers.

Analogous to the ^{1}H NMR spectra, the ^{13}C NMR spectrum at room temperature only shows broad and very weak signals while the spectrum recorded at low temperature shows sharp signals. At –30 °C, two well separated signals for the N–CH_3 groups are observed at δ = 33.9 and 33.2 ppm in accordance to the ^{1}H NMR spectroscopic data. Moreover, the characteristic downfield signal for the carbonyl carbon found at δ = 176.5 ppm for BM^{diPh}IK is no longer present in the product. Instead, a new signal at δ = 79.9 ppm is found, which is assigned to the alkoxide carbon.

As shortly mentioned above, the zinc-dimer [Zn$_2$(BM^{diPh}IA^{Et})$_2$Et$_2$] was hydrolyzed with a saturated aqueous NH$_4$Cl solution. Subsequent extraction with CH$_2$Cl$_2$ yielded H-BM^{diPh}IA^{Et} in 89 % yield. ^{1}H NMR analysis showed a pure product with a triplet at δ = 1.04 ppm and a quartet at δ = 2.75 ppm, indicating the ethyl-substituent (Figure S12). One singlet at δ = 3.32 ppm accounting for two N–CH_3 groups shows that the product is symmetric on the bridging carbon. ^{13}C NMR analysis confirmed the reduction of the carbonyl group, now showing a signal at δ = 72.8 ppm for the *C*OH (Figure S13). There is no indication for the transfer of ethyl ligands to other parts of the ligand; consequently 1,4-addition (*N*-alkylation) could be excluded.

Mechanistic Studies

To investigate the reaction mechanism of the 1,2-addition of Et$_2$Zn to the ketone in BM^{diPh}IK, the dark red intermediate (vide supra) was studied in more detail with NMR and EPR spectroscopy.

To be able to observe the reactive red intermediate species by NMR spectroscopy, the reaction mixture obtained from mixing Et$_2$Zn and BM^{diPh}IK at –95 °C in [D$_8$]toluene was transferred to a pre-cooled NMR tube and kept at –78 °C until it was transferred to the NMR spectrometer, which was pre-cooled to –60 °C. The sample was still dark red when moved into the NMR spectrometer and it gave rather clean ^{1}H and ^{13}C NMR spectra (Figure S9 and Figure 3, top). The ^{1}H NMR spectrum shows a quartet at δ = 0.32 ppm and a triplet at δ = 1.54 ppm assigned to the ethyl groups. The rather small shift compared to the authentic sample of Et$_2$Zn in [D$_8$]toluene at –60 °C, in which the signals appear at δ = 0.06 and 1.18 ppm (Figure S9, middle), indicates that both ethyl ligands are still bound to zinc. Furthermore, comparison to the ^{1}H NMR spectrum of the free BM^{diPh}IK

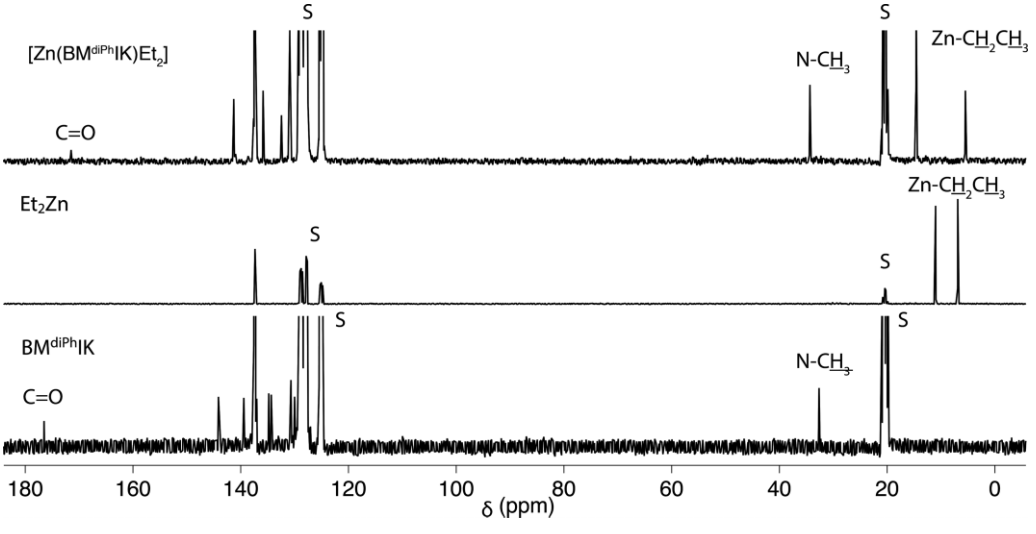

Figure 3. ^{13}C NMR spectra of [Zn(BM^{diPh}IK)Et$_2$] (top) and the starting materials Et$_2$Zn (middle) and BM^{diPh}IK (bottom) in [D$_8$]toluene recorded at –60 °C. S indicates the residual solvent peak.

ligand also shows minor shifts only, implying coordination of the ligand to the zinc center but no reaction on the ligand backbone.

In the ^{13}C NMR spectrum a downfield carbonyl signal is visible at δ = 171.5 ppm (δ =176.5 ppm in the free ligand), showing that the carbonyl in this intermediate species is still present (Figure 3, top). Additionally, the $BM^{diPh}IK$ methyl-substituent and zinc-bound ethyl ligands are observed at 5.48, 14.62, and 34.34 ppm, respectively. These NMR spectra support the idea that the dark red intermediate is the coordination compound $[Zn(BM^{diPh}IK)Et_2]$ as proposed in Scheme 2. This is in accordance with what was earlier proposed for similar reactions,[28,34] and the formation of this coordination compound is likely to be the first step in the reaction pathway towards the final Zn-alkoxide product.

Upon warming the NMR cavity from –60 °C to –40 °C a reaction started to occur. Over a period of 50 minutes a ^1H NMR spectrum was recorded every 10 min at –40 °C (Figure 4). During these 50 minutes the intensity of the $[Zn(BM^{diPh}IK)Et_2]$ signals gradually decreased and the intensity of the $[Zn_2(BM^{diPh}IA^{Et})_2Et_2]$ signals increased while the sum of the two species stayed the same (Figure S6). No significant amounts of other species were observed during this time interval, which indicates that intermediate species have a very short lifetime or are NMR silent, as could be the case with radical intermediates. In contrast to what Lewinski et al. observed in the reaction of Et_2Zn with dibenzoyl, there was no indication for the formation of aggregates in this reaction.[28]

For the strongly related reactions of e.g. α-diimines with alkylzinc reagents a SET radical mechanism is proposed.[41] However, the detection of any radical species with EPR spectroscopy during the course of the 1,2-addition reaction of Et_2Zn to $BM^{diPh}IK$ at various temperatures going gradually from 100 K to room temperature was not successful. This indicates that either no radical species are involved in this reaction or, more likely, that the radical intermediates are short lived and therefore exist only at low steady-state concentration, possibly reacting within the solvent cage.

In another attempt to determine the involvement of radical intermediates, a cold toluene solution containing 10 equivalents of DMPO (5,5-dimethyl-1-pyrroline-*N*-oxide) was added to a toluene solution of the dark red intermediate at –78 °C, this caused the mixture to turn colorless immediately without increasing the temperature. EPR analysis showed a signal with a g-value of 2.006, that is split into 6 lines with hyperfine coupling constants of A_N = 14.2 G and A_H = 40.2 G (Figure 5). This is in excellent agreement with literature data for the DMPO-ethyl radical.[62] The presence of the DMPO-ethyl radical shows that ethyl radicals are accessible from the reaction between Et_2Zn and $BM^{diPh}IK$.

However, the immediate disappearance of the red color upon the addition of the DMPO solution indicates that the DMPO does not trap the radicals that are present in solution but rather initiates the formation of ethyl radicals from $[Zn(BM^{diPh}IK)Et_2]$. The initiation of radical formation from Et_2Zn by a radical trap is not unprecedented. TEMPO, a different radi-

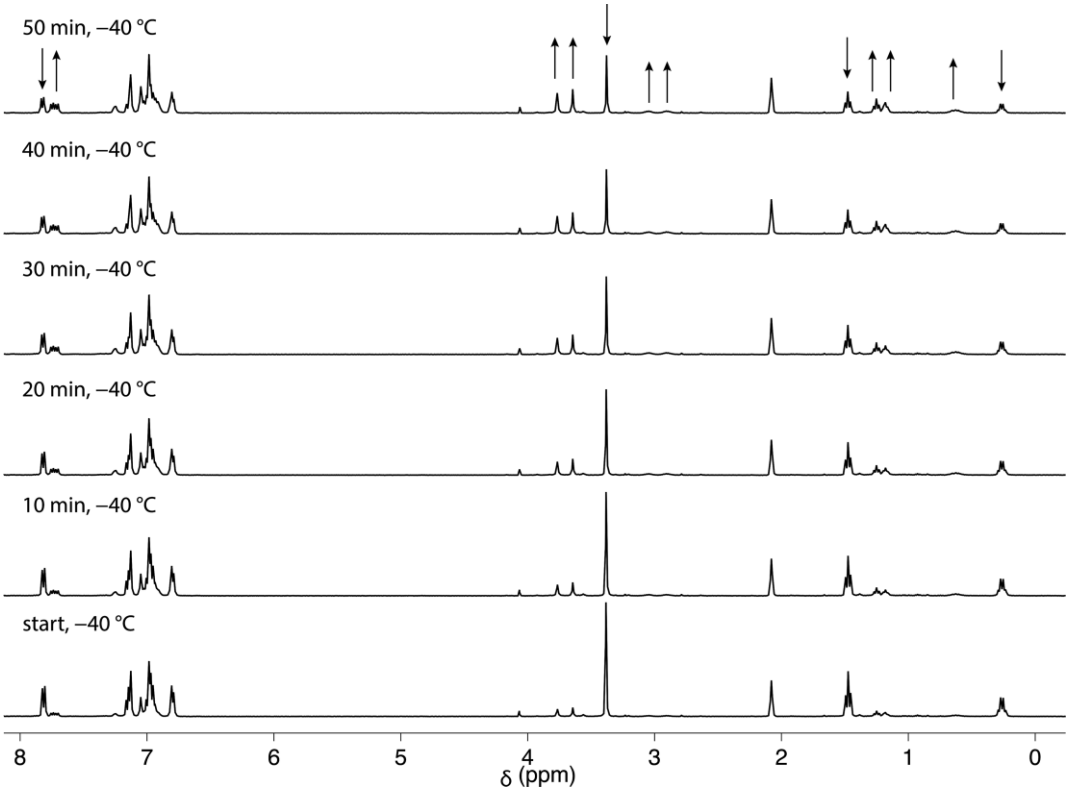

Figure 4. ^1H NMR spectral changes during the course of the reaction of $[Zn(BM^{diPh}IK)Et_2]$ towards $[Zn_2(BM^{diPh}IA^{Et})_2Et_2]$ recorded at –40 °C in $[D_8]$toluene. Increasing and decreasing signals upon progress of the reaction are shown with arrows.

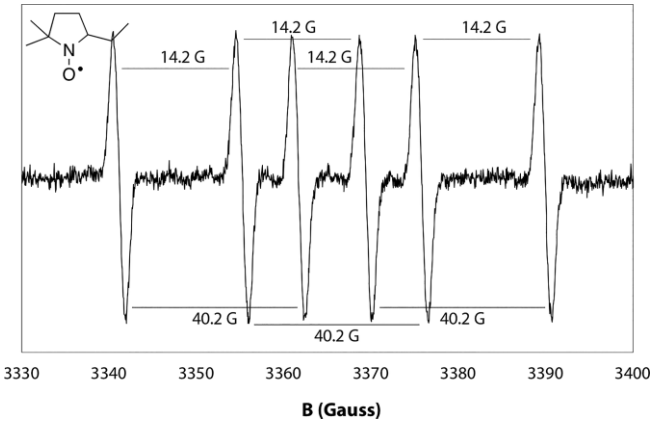

Figure 5. EPR spectrum of the reaction mixture of [Zn(BM^{diPh}IK)Et$_2$] with DMPO, recorded in toluene at ambient temperature.

cal trap, has been reported to react with Et_2Zn to afford both $[EtZn(TEMPO)]_n$ and $[Zn(TEMPO)_2]$ complexes along with ethane, ethylene, and TEMPOEt-Et.[43] Also, DMPO has been shown to react with Et_2Zn to form DMPO-Et radicals, albeit the reported reaction was performed in the presence of O_2.[63] In the blank experiment of Et_2Zn with DMPO, i.e. in the absence of BM^{diPh}IK, the same spectrum was obtained albeit in much lower intensity. Based on the higher intensity of the EPR signal in presence of BM^{diPh}IK, it was concluded that the presence of the ligand does enhance the radical transfer of the ethyl ligand.

Based on the experimental data, the mechanism as shown in Figure 6 is proposed for the reaction between Et_2Zn and BM^{diPh}IK. Initially, the experimentally detected coordination complex [Zn(BM^{diPh}IK)Et$_2$] forms, followed by the homolytic cleavage of the zinc–ethyl bond resulting in an ethyl-radical and a radical on the carbonyl in the BM^{diPh}IK ligand. These radical intermediates could not be detected, but the DMPO experiment suggests that ethyl radicals can be generated from [Zn(BM^{diPh}IK)Et$_2$]. The formed radical pair collapses within the solvent cage to form a C–C bond and transforms the carbonyl moiety in an alkoxide. Upon dimerization, to attain the tetrahedral geometry on the Zn-centers, the zinc dimer [Zn_2(BM^{diPh}IA^{Et})$_2$Et$_2$] is formed in which the formed alkoxide moieties bridge between two Zn centers and one ethyl ligand remains on each Zn-center. The spin density in the radical intermediate would be mainly located on the carbonyl resulting in the recombination of the radical pair at this position. This is fully consistent with previous studies on the reductive chemistry of the BM^{diPh}IK ligand and the corresponding zinc chloride complex for which a very similar radical intermediate is proposed.[40] The theoretical energies of formation of different reaction intermediates are indicated in Figure 6. The initial complexation of Et_2Zn by the BM^{diPh}IK ligand was found to be slightly endothermic by 7.5 kcal/mol, which appears inconsistent with the quantitative reaction observed experimentally. This is tentatively ascribed to solvent effects. The second step, i.e. the rate-limiting formation of the radical pair, is associated with a ΔH of 22.1 kcal/mol starting from the complex. These steps are followed by two more strongly exothermic bond-forming steps with ΔH of –32.0 and –26.4 kcal/mol, respectively, which are probably the driving forces in this reaction.

Conclusions

Here, the addition of Et_2Zn to the ketone in the BM^{diPh}IK ligand was shown to take place in a very selective manner. In contrast to reactions of α-diimines or α-iminoketones with Et_2Zn,[34,36] selective 1,2-addition was found to occur and no *N*-alkylation (1,4-addition) was observed. The final product was isolated and

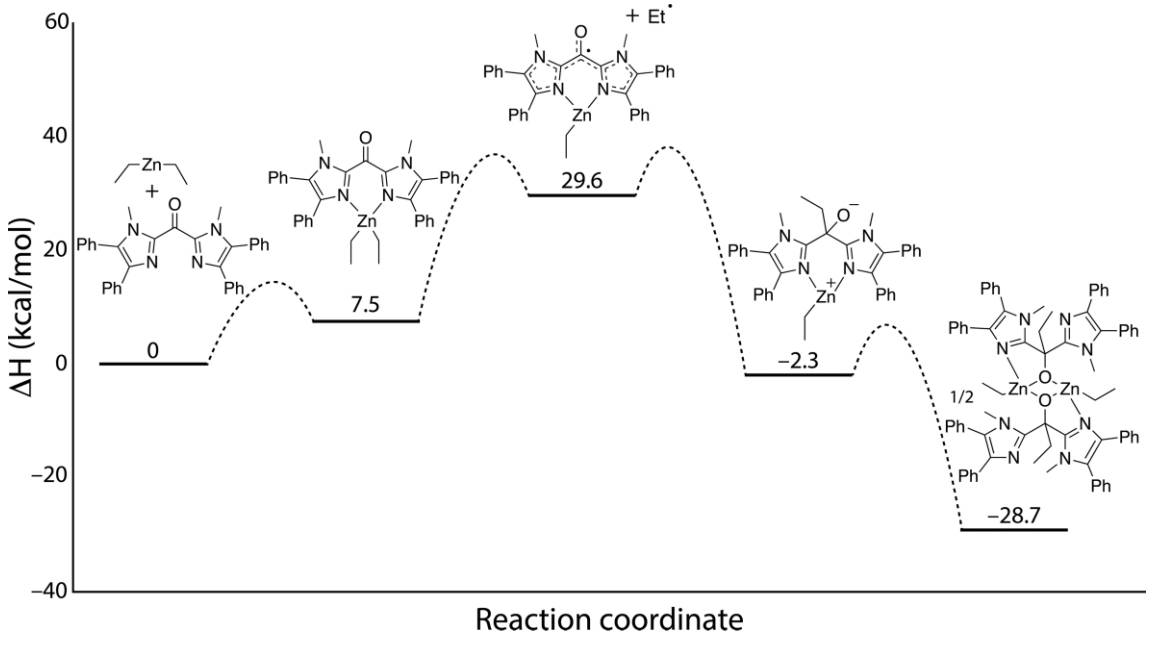

Figure 6. Energy diagram of the proposed radical reaction pathway for the 1,2-addition of Et_2Zn to the BM^{diPh}IK ketone ligand. Using the UBP86/6-31g* (C, H, N, and O) and LANL2DZ (Zn) DFT computational level. Transition states are not calculated; accordingly, the dotted connections between the intermediates do not indicate the energies of the transition states.

fully characterized as a C-alkylated binuclear zinc complex containing a planar centrosymmetric $Zn_2(\mu\text{-}O)_2$-motif.

Knowing from previous studies that BM^{diPh}IK can form rather stable radicals upon reduction,[40] this ligand was used to investigate the accessibility of a radical pathway for the alkylation of ketones. Although a polar mechanism cannot be excluded based on the experimental data shown here, the current study indicates the viability of a radical pathway. No radical intermediates have been detected, however the accessibility of ethyl-radicals was shown using DMPO as a radical trap. It is proposed that the radical intermediates recombine within the solvent cage, hampering their detection. The initially formed coordination compound, [Zn(BM^{diPh}IK)Et_2], that precedes ethyl-transfer, has been successfully characterized using low temperature NMR experiments. Additionally, DFT calculations confirmed the plausibility of the proposed radical pathway.

It is of interest to investigate the reactivity of BM^{diPh}IK with other alkylzinc reagents to see if this would allow the detection of more stable radical intermediates. Additionally, the ability to transfer the alkyl ligand to external reagents and to use catalytic amounts of BM^{diPh}IK would be of interest.

Experimental Section

All air-sensitive organic reactions, as well as the handling and synthesis of diethylzinc reagents, were carried out under an inert atmosphere of dry and oxygen-free N_2 using standard Schlenk techniques or were handled in an MBraun labmaster dp glovebox workstation. [D$_2$]CH_2Cl_2 was dried with CaH_2 and distilled under N_2 atmosphere prior to use. THF was distilled from sodium/benzophenone before use, distilled under N_2. Dry toluene and hexane were obtained from an mBraun MB SPS-800 solvent purification system and stored over 3 Å molecular sieves. [D$_8$]Toluene was dried with 3 Å molecular sieves. Solvents were degassed by bubbling N_2 through for ±30 min or by freeze-pump-thaw degassing prior to use. ^{1}H and ^{13}C{^{1}H}, and ^{1}H-^{13}C HSQC NMR spectra were recorded at 298 K on a Varian VNMRS400 or an Oxford NMR AS400 spectrometer at 400 MHz and 100 MHz, respectively. Chemical shifts are reported in ppm with respect to tetra methylsilane (TMS) based on the position of residual solvent peaks as reported by Fulmer et al.[64] ATR infrared spectra were recorded on a Perkin–Elmer Spectrum One FTIR spectrometer. ESI-MS spectra were recorded on a Waters LCT Premier XE KE317 Micromass Technologies spectrometer. Elemental microanalyses were carried out by the Mikroanalytischen Laboratorium Kolbe, Mulheim a.d. Ruhr, Germany. BM^{diPh}IK is synthesized according to literature procedure.[40] All other chemicals were commercially obtained and used as received. Caution: Et_2Zn used in the reactions described below are pyrophoric compounds reacting violently with oxygen and water. Special care must be taken when operating with these compounds.

[Zn(BM^{diPh}IK)Et_2]: Diethylzinc (1.0 M in [D$_8$]toluene, 0.10 mL, 0.10 mmol) was added to a frozen suspension of BM^{diPh}IK (50 mg, 0.10 mmol) in [D$_8$]toluene (2 mL) at –196 °C upon which the added drops froze instantaneously. The mixture was slowly melted, resulting in a clear dark red solution, which was transferred to an NMR tube and kept at –78 °C and transferred, as a dark red sample, to the pre-cooled NMR spectrometer at –60 °C. ^{1}H NMR (400 MHz, [D$_8$]toluene, –60 °C): δ = 7.84 (d, $^3J_{H,H}$ = 7.6 Hz, 4 H, *o*-Ph*H*), 7.15 (m, 6 H, Ph*H*), 6.95 (m, 6 H, Ph*H*), 6.75 (d, $^3J_{H,H}$ = 6.5 Hz, 4 H, *o*-Ph*H*), 3.34 (s, 6 H, NCH_3), 1.54 (t, $^3J_{H,H}$ = 7.7 Hz, 6 H, ZnCH$_2$CH_3), 0.32 (q, $^3J_{H,H}$ = 7.7 Hz, 4 H, ZnCH_2CH$_3$) ppm. ^{13}C NMR (101 MHz, [D$_8$]toluene, –60 °C): δ = 171.5, 141.3, 141.0, 135.8, 132.4, 130.9, 129.3, 128.9, 128.5, 128.3, 34.3, 14.6, 5.5 ppm (two signals are overlapping with residual toluene signals).

[Zn$_2$(BM^{diPh}IA^{Et})$_2$Et$_2$]: Diethylzinc (1.0 M in hexanes, 0.40 mL, 0.40 mmol) was added dropwise to a suspension of BM^{diPh}IK (199 mg, 0.402 mmol) in toluene (10 mL) at –78 °C to yield a dark red solution. During stirring for 1 h the reaction mixture stays dark red. The solution was warmed to room temperature for 1 h during which the mixture turns clear and colorless. Afterwards all volatiles were removed in vacuo to yield the crude product as a white powder, which was purified by crystallization from THF by slow vapor diffusion of hexanes (175 mg, 71 %). $C_{74}H_{72}N_8O_2Zn_2$ (1232.44): calcd. C 71.90, H 5.87, N 9.06; found C 72.11, H 6.03, N 8.97. ^{1}H NMR (400 MHz, [D$_8$]toluene, –30 °C): δ = 7.74 (d, $^3J_{H,H}$ = 7.8 Hz, 4 H, *o*-Ph*H*), 7.70 (d, $^3J_{H,H}$ = 7.5 Hz, 4 H, *o*-Ph*H*), 7.25 ("d", $^3J_{H,H}$ = 4.7 Hz, 4 H, *o*-Ph*H*), 7.12 (s, 3 H), 7.06–6.89 (m, 21 H), 6.84 (d, $^3J_{H,H}$ = 7.1 Hz, 4 H, *o*-Ph*H*), 3.76 (s, 6 H, NCH_3), 3.65 (s, 6 H, NCH_3), 3.03 [ABX$_3$, $^2J_{H,H}$ = 13.3 Hz, 2 H, C(O)CH_2CH$_3$], 2.89 [ABX$_3$, $^2J_{H,H}$ = 13.3 Hz, 2 H, C(O)CH_2CH$_3$], 1.23 (t, $^3J_{H,H}$ = 8.0 Hz, 6 H, ZnCH$_2$CH_3), 1.18 [t, $^3J_{H,H}$ = 7.2 Hz, 6 H, C(O)CH$_2$CH_3], 0.58 (ABX$_3$, $^2J_{H,H}$ = 12.9 Hz, 2 H, ZnCH_2CH$_3$), 0.53 (ABX$_3$, $^2J_{H,H}$ = 12.9 Hz, 2 H, ZnCH_2CH$_3$) ppm. ^{13}C NMR (101 MHz, [D$_8$]toluene, –30 °C): δ = 157.8, 150.0, 136.1, 135.9, 133.8, 133.6, 132.0, 131.8, 131.4, 131.2, 129.9, 129.8, 128.9, 128.2, 128.0, 127.3, 126.0, 79.9, 35.7, 33.9, 33.2, 12.8, 9.0, 2.3 ppm (some signals are overlapping with the toluene signals). IR (ATR): $\tilde{\nu}$ = 3054.3 (w), 3032.6 (w), 3005.1 (w), 2971.3 (w), 2929.2 (w), 2882.5 (w), 2844.0 (w), 1602.0 (m), 1504.2 (m), 1465.9 (m), 1443.1 (m), 1394.2 (m), 1386.2 (m), 1326.6 (w), 1290.0 (w), 1245.9 (w), 1232.0 (w), 1170.0 (w), 1134.2 (m), 1079.4 (m), 1070.4 (m), 1025.0 (m), 981.42 (m), 916.9 (m), 889.5 (m), 774.75 (s), 749.57 (m), 695.72 (s), 600.75 (m), 544.35 (m), 506.1 (m) cm^{-1}. ESI-MS (THF/CH_2Cl_2/formic acid): *m/z* = 1111.4349 [Zn(BM^{diPh}IA^{Et})$_2$ – H$^+$]$^+$, calcd. 1111.4365, 1207.3925 [Zn$_2$(BM^{diPh}IA^{Et})$_2$Et$_2$ – Et$^-$]$^+$, calcd. 1207.3948. X-ray crystal structure determination: $C_{74}H_{72}N_8O_2Zn_2$, *Fw* = 1236.13, colorless plate, 0.19 × 0.12 × 0.03 mm^3, monoclinic, $P2_1/c$ (no. 14), *a* = 13.2084(6), *b* = 17.9543(6), *c* = 13.4432(6) Å, β = 107.174(2)°, *V* = 3045.9(2) Å^3, *Z* = 2, D_x = 1.348 g/cm^3, μ = 0.84 mm^{-1}. 42520 Reflections were measured on a Bruker Kappa ApexII diffractometer with sealed tube and Triumph monochromator (λ = 0.71073 Å) at a temperature of 150(2) K up to a resolution of (sin $\theta/\lambda)_{max}$ = 0.65 Å^{-1}. The Eval15 software[65] was used for the integration of the intensities. Multiscan absorption correction and scaling was performed with SADABS[66] (correction range 0.60–0.75). 6990 Reflections were unique (R_{int} = 0.052), of which 4883 were observed [$I > 2\sigma(I)$]. The structure was solved with Patterson superposition methods using SHELXT.[67] Least-squares refinement was performed with SHELXL-2014[68] against F^2 of all reflections. Non-hydrogen atoms were refined freely with anisotropic displacement parameters. The metal-bound ethyl group was refined with a disorder model (occupancy 0.8:0.2). Hydrogen atoms were introduced in calculated positions and refined with a riding model. 397 Parameters were refined with 2 restraints (distances and angles in the disordered moiety). *R1/wR2* [$I > 2\sigma(I)$]: 0.0432/0.1008. *R1/wR2* [all refl.]: 0.0750/0.1145. *S* = 1.031. Residual electron density between –0.33 and 0.51 e/Å^3. Geometry calculations and checking for higher symmetry were performed with the PLATON program.[69]

CCDC 1582913 {for [Zn$_2$(BM^{diPh}IA^{Et})$_2$Et$_2$]} contains the supplementary crystallographic data for this paper. These data can be obtained free of charge from The Cambridge Crystallographic Data Centre.

H-BM^{diPh}IA^{Et}: [Zn$_2$(BM^{diPh}IA^{Et})$_2$Et$_2$] (58.5 mg, 0.0473 mmol) was hydrolyzed by the addition of a saturated NH_4Cl solution (5 mL). The

obtained suspension was extracted with CH_2Cl_2 (3 × 10 mL). The yellow organic layers were collected and dried with $MgSO_4$, filtered and all volatiles were removed in vacuo yielding the product as yellow solid (44.4 mg, 89 %). ^{1}H NMR (400 MHz, [D$_8$]toluene, –30 °C): δ = 7.50–7.43 (m, 10 H, Ph*H*), 7.33–7.31 (m, 4 H, Ph*H*), 7.23–7.19 (m, 4 H, Ph*H*), 7.16–7.12 (m, 2 H, Ph*H*), 5.82 (s, 1 H, O*H*), 3.32 (s, 6 H, NCH_3), 2.75 [q, $^3J_{H,H}$ = 7.4 Hz, 2 H, C(OH)CH_2CH$_3$], 1.04 [t, $^3J_{H,H}$ = 7.4 Hz, 3 H, C(OH)CH$_2$CH_3] ppm. ^{13}C NMR (101 MHz, [D]chloroform$_1$, 25 °C): δ = 147.5, 135.3, 134.6, 131.3, 131.1, 130.7, 129.1, 128.9, 128.3, 126.8, 126.4, 72.8, 32.1, 31.9, 7.7 ppm. IR (ATR): $\tilde{\nu}$ = 3405.2 (br., w), 3056.5 (w), 3029.0 (w), 2961.2 (w), 2937.4 (w), 1602.8 (m), 1505.5 (m), 1443.0 (m), 1386.8 (m), 1356.0 (m), 1320.8 (m), 1231.7 (w), 1179.0 (w), 1134.6 (m), 1072.3 (m), 1025.0 (m), 967.33 (m), 917.55 (w), 841.25 (w), 774.07 (s), 747.7 (w), 696.16 (s), 649.62 (w), 544.11 (m) cm^{-1}. ESI-MS (THF/CH_2Cl_2/formic acid): *m*/*z* = 525.2654 [(H-BM^{diPh}IA^{Et}) + H$^+$]$^+$, calcd. 525.2654.

Radical Trapping with DMPO: Diethylzinc (1.0 M in toluene, 0.10 mL, 0.10 mmol) was added dropwise to a yellow suspension of BM^{diPh}IK (50 mg, 0.10 mmol) in toluene (10 mL) at –78 °C to yield a dark red solution. A part of this dark red solution (0.15 mL) is transferred to a cold EPR tube and a cold solution containing 10 equiv. of DMPO (0.1 M in toluene, 0.15 mL) is added upon which the red color immediately disappeared resulting in a colorless solution.

Computational Details: DFT results were obtained using the Gaussian 09 software package,[70] using the UBP86 functional and the 6-31g* basis set on C, H, N, and O and LANL2DZ on Zn. Frequency analyses were performed on all calculations.

Acknowledgments

The authors would like to thank the Dutch National Research School Combination-Catalysis Controlled by Chemical Design (NRSC-Catalysis) for financial support. M.-E. M. acknowledges funding from the European Union Seventh Framework Programme FP7/2007-2013 under grant agreement PIIF-GA-2012-327306 (IIF-Marie Curie grant) and Utrecht University (Tenure-track grant, Sectorplan Natuur- en Scheikunde). The DFT work was carried out on the Dutch national e-infrastructure with the support of the SURF Foundation. The X-ray diffractometer has been financed by the Netherlands Organization for Scientific Research (NWO).

Keywords: Zinc · Radical reactions · Reactive intermediates · Homogeneous catalysis

[1] A. B. Charette in *The Chemistry of Organozinc Compounds* (Eds.: Z. Rappoport, I. Marek), John Wiley & Sons, Chichester, UK, **2006**, pp. 237–286.
[2] E.-I. Negishi, Q. Hu, Z. Huang, G. Wang, N. Yin in *The Chemistry of Organozinc Compounds* (Eds.: Z. Rappoport, I. Marek), John Wiley & Sons, Chichester, UK, **2006**, pp. 457–553.
[3] T. Harada in *The Chemistry of Organozinc Compounds* (Eds.: Z. Rappoport, I. Marek), John Wiley & Sons, Chichester, UK, **2006**, pp. 685–711.
[4] AkzoNobel Functional Chemicals, *Zinc Alkyls in Organic Synthesis* **2008**.
[5] E. Lorthiois, C. Meyer in *The Chemistry of Organozinc Compounds* (Eds.: Z. Rappoport, I. Marek), John Wiley & Sons, Chichester, UK, **2006**, pp. 863–978.
[6] T. Akindele, K. Yamada, K. Tomioka, *Acc. Chem. Res.* **2009**, *42*, 345–355.
[7] K. Yamada, K. Tomioka, *Chem. Rec.* **2015**, *15*, 854–871.
[8] M. Kubisiak, K. Zelga, W. Bury, I. Justyniak, K. Budny-Godlewski, Z. Ochal, J. Lewiński, *Chem. Sci.* **2015**, *6*, 3102–3108.
[9] O. Riant, J. Hannedouche, *Org. Biomol. Chem.* **2007**, *5*, 873–888.
[10] A. V. R. Madduri, S. R. Harutyunyan, A. J. Minnaard, *Drug Discovery Today Technol.* **2013**, *10*, e21–e27.
[11] L. Pu, H.-B. Yu, *Chem. Rev.* **2001**, *101*, 757–824.
[12] R. Noyori, M. Kitamura, *Angew. Chem. Int. Ed. Engl.* **1991**, *30*, 49–69; *Angew. Chem.* **1991**, *103*, 34.
[13] J. M. Betancort, C. García, P. J. Walsh, *Synlett* **2004**, *5*, 749–760.
[14] P. G. Cozzi, R. Hilgraf, N. Zimmermann, *Eur. J. Org. Chem.* **2007**, *2007*, 5969–5994.
[15] A. Chieffi, K. Kamikawa, J. Åhman, J. M. Fox, S. L. Buchwald, *Org. Lett.* **2001**, *3*, 1897–1900.
[16] D. J. Ramón, M. Yus, *Tetrahedron Lett.* **1998**, *39*, 1239–1242.
[17] V. J. Forrat, O. Prieto, D. J. Ramón, M. Yus, *Chem. Eur. J.* **2006**, *12*, 4431–4445.
[18] C. García, P. J. Walsh, *Org. Lett.* **2003**, *5*, 3641–3644.
[19] A. Hui, J. Zhang, J. Fan, Z. Wang, *Tetrahedron: Asymmetry* **2006**, *17*, 2101–2107.
[20] S.-J. Jeon, P. J. Walsh, *J. Am. Chem. Soc.* **2003**, *125*, 9544–9545.
[21] S.-J. Jeon, H. Li, P. J. Walsh, *J. Am. Chem. Soc.* **2005**, *127*, 16416–16425.
[22] S.-J. Jeon, H. Li, C. García, L. K. LaRochelle, P. J. Walsh, *J. Org. Chem.* **2005**, *70*, 448–455.
[23] H. Li, C. García, P. J. Walsh, *Proc. Natl. Acad. Sci. USA* **2004**, *101*, 5425–5427.
[24] D. J. Ramón, M. Yus, *Angew. Chem. Int. Ed.* **2004**, *43*, 284–287; *Angew. Chem.* **2004**, *116*, 286.
[25] M. Hatano, T. Mizuno, K. Ishihara, *Tetrahedron* **2011**, *67*, 4417–4424.
[26] P. I. Dosa, G. C. Fu, *J. Am. Chem. Soc.* **1998**, *120*, 445–446.
[27] M. Hatano, T. Miyamoto, K. Ishihara, *Org. Lett.* **2007**, *9*, 4535–4538.
[28] I. Dranka, M. Kubisiak, I. Justyniak, M. Lesiuk, D. Kubicki, J. Lewiński, *Chem. Eur. J.* **2011**, *17*, 12713–12721.
[29] C. M. Binder, B. Singaram, *Org. Prep. Proced. Int.* **2011**, *43*, 139–208.
[30] M. Hatano, T. Mizuno, K. Ishihara, *Synlett* **2010**, 2024–2028.
[31] M. Hatano, T. Mizuno, K. Ishihara, *Chem. Commun.* **2010**, *46*, 5443–5445.
[32] J. T. B. H. Jastrzebski, J. Boersma, G. van Koten in *The Chemistry of Organozinc Compounds* (Eds.: Z. Rappoport, I. Marek), John Wiley & Sons, Chichester, UK, **2006**, pp. 31–135.
[33] C. Lichtenberg, J. Engel, T. P. Spaniol, U. Englert, G. Raabe, J. Okuda, *J. Am. Chem. Soc.* **2012**, *134*, 9805–9811.
[34] M. R. P. van Vliet, J. T. B. H. Jastrzebski, G. van Koten, K. Vrieze, A. L. Spek, *J. Organomet. Chem.* **1983**, *251*, c17–c21.
[35] M. R. P. van Vliet, G. van Koten, P. Buysingh, J. T. B. H. Jastrzebski, A. L. Spek, *Organometallics* **1987**, *6*, 537–546.
[36] E. Wissing, E. Rijnberg, P. A. van der Schaaf, K. van Gorp, J. Boersma, G. van Koten, *Organometallics* **1994**, *13*, 2609–2615.
[37] E. Wissing, J. T. B. H. Jastrzebski, J. Boersma, G. van Koten, *J. Organomet. Chem.* **1993**, *459*, 11–16.
[38] P. J. Bailey, C. M. Dick, S. Fabre, S. Parsons, L. J. Yellowlees, *Dalton Trans.* **2006**, 1602–1610.
[39] W. Kaim, *Acc. Chem. Res.* **1985**, *18*, 160–166.
[40] E. Folkertsma, S. H. Benthem, L. Witteman, C. A. M. R. van Slagmaat, M. Lutz, R. J. M. Klein Gebbink, M.-E. Moret, *Dalton Trans.* **2017**, *46*, 6177–6182.
[41] M. Kaupp, H. Stoll, H. Preuss, W. Kaim, T. Stahl, G. van Koten, E. Wissing, W. J. J. Smeets, A. L. Spek, *J. Am. Chem. Soc.* **1991**, *113*, 5606–5618.
[42] Ł. Mąkolski, K. Zelga, R. Petrus, D. Kubicki, P. Zarzycki, P. Sobota, J. Lewiński, *Chem. Eur. J.* **2014**, *20*, 14790–14799.
[43] K. Budny-Godlewski, D. Kubicki, I. Justyniak, J. Lewiński, *Organometallics* **2014**, *33*, 5093–5096.
[44] K. Robinson, G. V. Gibbs, P. H. Ribbe, *Science* **1971**, *172*, 567–570.
[45] N. V. Kulkarni, A. Das, S. G. Ridlen, E. Maxfield, V. A. K. Adiraju, M. Yousufuddin, H. V. R. Dias, *Dalton Trans.* **2016**, *45*, 4896–4906.
[46] J. T. B. H. Jastrzebski, J. Boersma, G. van Koten, W. J. J. Smeets, A. L. Spek, *Recl. Trav. Chim. Pays-Bas* **1988**, *107*, 263–266.
[47] Y. Wang, W. Zhao, D. Liu, S. Li, X. Liu, D. Cui, X. Chen, *Organometallics* **2012**, *31*, 4182–4190.
[48] D. Walther, T. Döhler, N. Theyssen, H. Görls, *Eur. J. Inorg. Chem.* **2001**, 2049–2060.
[49] A. L. Johnson, N. Hollingsworth, G. Kociok-Köhn, K. C. Molloy, *Inorg. Chem.* **2008**, *47*, 12040–12048.
[50] J. Hunger, S. Blaurock, J. Sieler, *Z. Anorg. Allg. Chem.* **2005**, *631*, 472–478.

[51] C. Di Iulio, M. Middleton, G. Kociok-Köhn, M. D. Jones, A. L. Johnson, *Eur. J. Inorg. Chem.* **2013**, *2013*, 1541–1554.
[52] R. Duchateau, W. J. van Meerendonk, S. Huijser, B. B. P. Staal, M. A. van Schilt, G. Gerritsen, A. Meetsma, C. E. Koning, M. F. Kemmere, J. T. F. Keurentjes, *Organometallics* **2007**, *26*, 4204–4211.
[53] I. Siewert, M. Sietzen, S. Dechert, S. Demeshko, *Eur. J. Inorg. Chem.* **2013**, *2013*, 3689–3698.
[54] D. J. Darensbourg, J. R. Wildeson, J. C. Yarbrough, J. H. Reibenspies, *J. Am. Chem. Soc.* **2000**, *122*, 12487–12496.
[55] J. Lewiński, W. Śliwiński, M. Dranka, I. Justyniak, J. Lipkowski, *Angew. Chem. Int. Ed.* **2006**, *45*, 4826–4829; *Angew. Chem.* **2006**, *118*, 4944.
[56] R. Petrus, P. Sobota, *Organometallics* **2012**, *31*, 4755–4762.
[57] T. K. Sen, A. Mukherjee, A. Modak, S. K. Mandal, D. Koley, *Dalton Trans.* **2013**, *42*, 1893–1904.
[58] J. Y. Li, C. Y. Li, W. J. Tai, C. H. Lin, B. T. Ko, *Inorg. Chem. Commun.* **2011**, *14*, 1140–1144.
[59] M. Kitamura, S. Suga, M. Niwa, R. Noyori, *J. Am. Chem. Soc.* **1995**, *117*, 4832–4842.
[60] C. Bolm, J. Müller, G. Schlingloff, M. Zehnder, M. Neuburger, *J. Chem. Soc., Chem. Commun.* **1993**, 182–183.
[61] K. Nakano, K. Nozaki, T. Hiyama, *J. Am. Chem. Soc.* **2003**, *125*, 5501–5510.
[62] G. R. Buettner, *Free Radical Biol. Med.* **1987**, *3*, 259–303.
[63] J. Maury, L. Feray, S. Bazin, J.-L. Clément, S. R. A. Marque, D. Siri, M. P. Bertrand, *Chem. Eur. J.* **2011**, *17*, 1586–1595.
[64] G. R. Fulmer, A. J. M. Miller, N. H. Sherden, H. E. Gottlieb, A. Nudelman, B. M. Stoltz, J. E. Bercaw, K. I. Goldberg, *Organometallics* **2010**, *29*, 2176–2179.
[65] A. M. M. Schreurs, X. Xian, L. M. J. Kroon-Batenburg, *J. Appl. Crystallogr.* **2010**, *43*, 70–82.
[66] G. M. Sheldrick, *SADABS and TWINABS*; University of Göttingen, Germany, **2008**.
[67] G. M. Sheldrick, *Acta Crystallogr., Sect. A* **2015**, *71*, 3–8.
[68] G. M. Sheldrick, *Acta Crystallogr., Sect. C* **2015**, *71*, 3–8.
[69] A. L. Spek, *Acta Crystallogr., Sect. D* **2009**, *65*, 148–155.
[70] M. J. Frisch, G. W. Trucks, H. B. Schlegel, G. E. Scuseria, M. A. Robb, J. R. Cheeseman, G. Scalmani, V. Barone, B. Mennucci, G. A. Petersson, H. Nakatsuji, M. Caricato, X. Li, H. P. Hratchian, A. F. Izmaylov, J. Bloino, G. Zheng, J. L. Sonnenberg, M. Hada, M. Ehara, K. Toyota, R. Fukuda, J. Hasegawa, M. Ishida, T. Nakajima, Y. Honda, O. Kitao, H. Nakai, T. Vreven, J. A. Montgomery Jr., J. E. Peralta, F. Ogliaro, M. Bearpark, J. J. Heyd, E. Brothers, K. N. Kudin, V. N. Staroverov, R. Kobayashi, J. Normand, K. Raghavachari, A. Rendell, J. C. Burant, S. S. Iyengar, J. Tomasi, M. Cossi, N. Rega, J. M. Millam, M. Klene, J. E. Knox, J. B. Cross, V. Bakken, C. Adamo, J. Jaramillo, R. Gomperts, R. E. Stratmann, O. Yazyev, A. J. Austin, R. Cammi, C. Pomelli, J. W. Ochterski, R. L. Martin, K. Morokuma, V. G. Zakrzewski, G. A. Voth, P. Salvador, J. J. Dannenberg, S. Dapprich, A. D. Daniels, Ö. Farkas, J. B. Foresman, J. V. Ortiz, J. Cioslowski, D. J. Fox, *Gaussian 09, Revision D.01*; Gaussian, Inc., Wallingford CT, **2013**.

Received: November 22, 2017